JACS
JOURNAL OF THE AMERICAN CHEMICAL SOCIETY
ARTICLE
pubs.acs.org/JACS

Examining the Effect of the Dipole Moment on Charge Separation in Donor−Acceptor Polymers for Organic Photovoltaic Applications

Bridget Carsten,[†] Jodi M. Szarko,[∥] Hae Jung Son,[†] Wei Wang,[†] Luyao Lu,[†] Feng He,[†] Brian S. Rolczynski,[‡,§,∥] Sylvia J. Lou,[‡,∥] Lin X. Chen,[*,‡,§,∥] and Luping Yu[*,†,§]

[†]Department of Chemistry and the James Franck Institute, The University of Chicago, 929 East 57th Street, Chicago, Illinois 60637, United States

[‡]Department of Chemistry, and [§]ANSER Center, Northwestern University, 2145 Sheridan Road, Evanston, Illinois 60208, United States

[∥]The Chemical Sciences and Engineering Division, Argonne National Laboratory, 9700 South Cass Avenue, Argonne, Illinois 60439, United States

S *Supporting Information*

ABSTRACT: A new low band gap copolymer **PBB3** containing [6,6′]bi[thieno[3,4-*b*]thiophenyl]-2,2′-dicarboxylic acid bis-(2-butyloctyl) ester (BTT) and 4,8-bis(2-butyloctyl)benzo[1,2-*b*:4,5-*b*′]dithiophene (BDT) units was synthesized and tested for solar cell efficiency. **PBB3** showed a broad absorbance in the near-IR region with a substantially red-shifted (by more than 100 nm) λ_{max} at 790 nm as compared to the **PTB** series of polymers, which have been previously reported. The **PBB3** polymer also showed both a favorable energy level match with PCBM (with a LUMO energy level of −3.29 eV) and a favorable film domain morphology as evidenced by TEM images. Despite these seemingly optimal parameters, a bulk heterojunction (BHJ) photovoltaic device fabricated from a blend of **PBB3** and $PC_{71}BM$ showed an overall power conversion efficiency (PCE) of only 2.04% under AM 1.5G/100 mW cm^{-2}. The transient absorption spectra of **PBB3** showed the absence of cationic and pseudo charge transfer states that were observed previously in the **PTB** series polymers, which were also composed of alternating thienothiophene (TT) and BDT units. We compared the spectral features and electronic density distribution of **PBB3** with those of **PTB2**, **PTB7**, and **PTBF2**. While **PTB2** and **PTB7** have substantial charge transfer characteristics and also relatively large local internal dipoles through BDT to TT moieties, **PTBF2** and **PBB3** have minimized internal dipole moments due to the presence of two adjacent TT units (or two opposing fluorine atoms in **PTBF2**) with opposite orientations or internal dipoles. **PBB3** showed a long-lived excitonic state and the slowest electron transfer dynamics of the series of polymers, as well as the fastest recombination rate of the charge-separated (CS) species, indicating that electrons and holes are more tightly bound in these species. Consequently, substantially lower degrees of charge separation were observed in both **PBB3** and **PTBF2**. These results show that not only the energetics but also the internal dipole moment along the polymer chain may be critical in maintaining the pseudocharge transfer characteristics of these systems, which were shown to be partially responsible for the high PCE device made from the **PTB** series of low band gap copolymers.

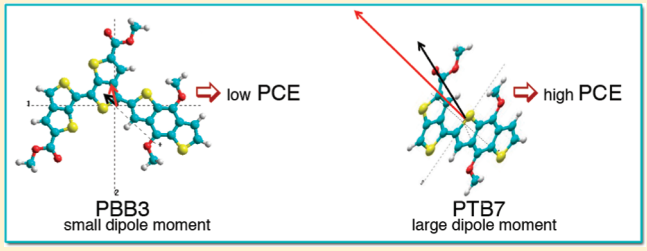

INTRODUCTION

Organic photovoltaic (OPV) materials represent a highly abundant, low-cost alternative to their inorganic counterparts for conversion of solar energy into electricity in solar cells. Organic materials are flexible and can be easily processed via facile, low-cost processing techniques in solution.[1,2] Despite their numerous advantages, however, the field of organic photovoltaics is still in its early stages. The power conversion efficiency (PCE) of organic solar cells with large areas is still much lower than that of solar cells using inorganic materials, which limits their commercial viability. It is a consensus that organic materials providing PCE of greater than 10% are needed to make them commercially viable. Thus, extensive research effort is focused on the design of new materials with optimized structure and properties, and the development of device preparation conditions to achieve this goal.

The conversion process of photons into electric energy in OPV devices consists of a series of steps.[3] First, when chromophores absorb photons possessing energy greater than their band gaps, an exciton is generated. The exciton then diffuses to the donor/acceptor interface where electron transfer to acceptor material, typically a fullerene[4] such as PCBM, may occur to form bound electron−hole pairs (charge transfer complexes). Charge transfer complexes must then be further separated into free charge carriers to be transported to cathode and anode to generate the current through the device.

One limitation in organic materials is that the exciton lifetime is typically very short; thus the maximum exciton diffusion length

Received: September 13, 2011
Published: November 12, 2011

ACS Publications © 2011 American Chemical Society

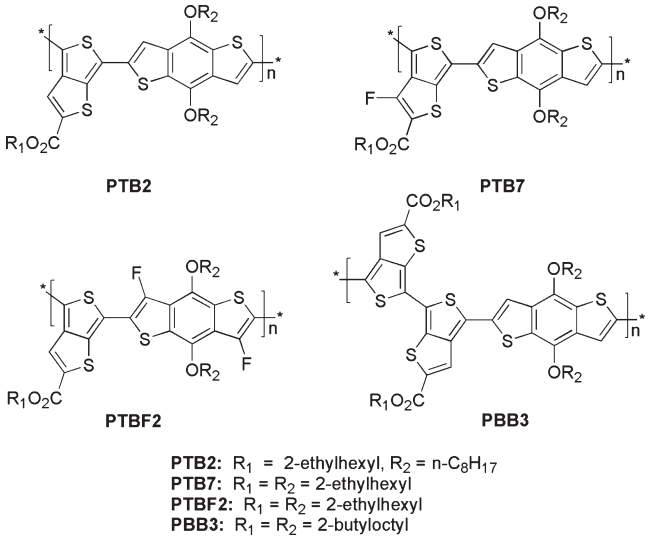

Figure 1. Structures of **PTB2**, **PTB7**, **PTBF2**, and **PBB3** polymers.

is typically only around 10 nm. Additionally, as Durrant and coworkers showed,[3,5] the process of interfacial charge separation is more complex than a simplified model assumes, involving Coulombically bound electron−hole pairs; thus, an adequate driving force for charge separation must exist for full separation of electron and hole. Similarly, adequate device architecture must exist for excitons to diffuse to the donor−acceptor interface. Finally, the polymer films must be thin enough to allow adequate charge transfer to electrodes. The concept of the bulk heterojunction solar cell was developed to address many of these issues. Through formation of interpenetrating networks of donor (polymer) and acceptor (typically fullerene) materials with nanoscale phase separation, the donor and acceptor domain sizes could be limited to the approximate exciton diffusion length of around 10 nm, and the degree of interfacial interaction between donor and acceptor could be rendered more optimal. The BHJ architecture[1,6−9] has been extensively studied in OPV devices, employing a blend of donor polymer and PCBM acceptor.

Development of new polymers has focused on the rational design of low band gap polymers.[2,10−13] A common strategy in lowering the band gap has been to incorporate the "push−pull" or "donor−acceptor (D−A)" concept into the polymer backbone.[14] This consists of alternating electron-rich with electron-deficient comonomers. The result of this is 2-fold. First, the band gap is effectively lowered by matching the LUMO of the donor component to near the HOMO of the acceptor component. Second, the push−pull nature of the alternating electron-rich/electron-deficient units facilitates intrachain charge transfer.[15,16]

Previously, our group has reported power conversion efficiencies (PCEs) close to 8% in photovoltaic devices based on the **PTB** series of polymers containing the thieno[3,4-*b*]thiophene (TT) and benzodithiophene (BDT) monomers.[17−20] As our previous results indicated,[21] the incorporation of the electron-deficient TT moiety effectively reduced the polymer band gap. It was found that fluorine substitution of the TT component lowered both HOMO and LUMO energy levels concomitantly, thus maintaining the low band gap while optimizing open circuit voltage.[22,23] In this work, we attempted to further tune the band gap closer to 1.5 eV and energy levels of the polymer by introducing

Scheme 1. Synthesis of 4,4′-Dibromo-[6,6′]bi[thieno[3,4-*b*]-thiophenyl]-2,2′-dicarboxylic Acid Bis-(2-butyl-octyl) Ester and PBB3 Polymer

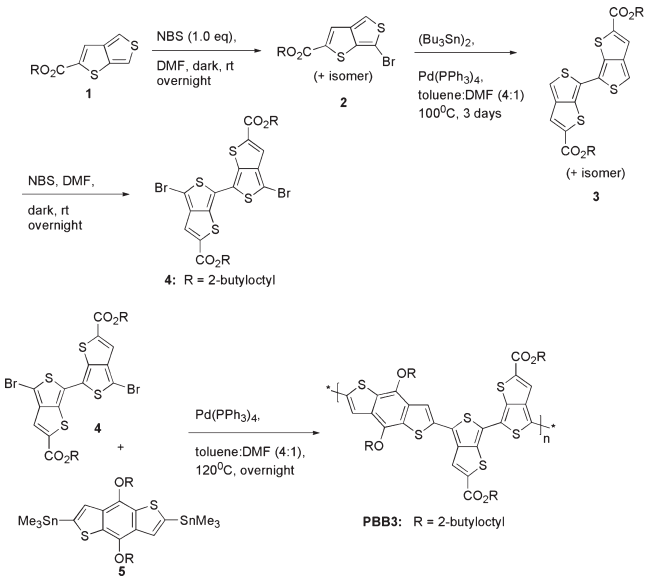

the dimer of thieno[3,4-*b*]thiophene, [6,6′]bi[thieno[3,4- *b*]thiophenyl]-2,2′-dicarboxylic acid bis-(2-butyl-octyl) ester (BTT).

A new low band gap polymer (**PBB3**) was thus synthesized (Figure 1). We reasoned that the introduction of a second TT moiety to the polymer backbone may lower the LUMO energy level even further, thus further reducing the band gap of the system.[10,15] It was found, however, that the introduction of a second TT unit as seen in the dimer had a detrimental effect on the PCE, although a host of physical properties of **PBB3** were seemly optimized. After examining all electronic and morphological features of this polymer, we rationalize this effect based on the change in net local dipole moment. Comparison of detailed transient absorption spectra of this polymer and several previously reported systems including **PTB2**,[19] **PTB7**,[17] and **PTBF2**[24] (Figure 1) shows that the poor efficiency may be due to a higher degree of exciton recombination due to the presence of a minimized dipole moment. The results from this work on a series of low band gap polymers shed some light into the validity of the concept of donor−acceptor copolymers for solar cell applications.

RESULTS AND DISCUSSION

Synthesis of PBB3. The **PBB3** polymer was synthesized via the Stille polycondensation method[25] from the corresponding dibromo monomer **4** and ditin monomer **5** as shown in Scheme 1 using $Pd(PPh_3)_4$ as catalyst in a refluxing mixed solvent system of 4:1 toluene:DMF.

Syntheses of compounds **1** and **5** were carried out as previously reported[19,26] with the modification that the 2-butyloctyl instead of 2-ethylhexyl side chain was incorporated. Compound **1** was then converted to **2** by monobromination using extremely slow addition (over 6 h) of 1 equiv of *N*-bromosuccinimide (NBS). This resulted in a mixture of isomers in an approximate ratio of 7:3 as determined from the HNMR spectrum, which were used as obtained in the next step. The monobrominated TT

compound **2** was then homo-coupled to produce the TT dimer **3** using a modified Stille condensation procedure employing $(SnBu_3)_2$, catalyzed by $Pd(PPh_3)_4$ in a heated 4:1 mixture of toluene:DMF. The two major isomers formed in this step were then easily separated by silica gel column chromatography, resulting in isomerically pure **3** as shown. The pure isomer of dimer **3** was then dibrominated by NBS to form monomer **4**.

CHARACTERIZATION OF THE POLYMER

Optical Absorption Spectroscopy. **PBB3** exhibited superior optical absorption properties as compared to the polymer **PTB2** and **PTB7** with only one TT unit in terms of harvesting near-IR solar photons. The solution and film optical absorption spectra for **PBB3** are shown in Figure 2 with solution spectra of **PTB2**, **PTB7**, and **PTBF2** for comparison. The relevant data are summarized in Table 1 with comparison data for **PTB2**, **PTB7**, and **PTBF2**. The optical band gap was calculated from the absorption onset (λ_{onset}). The solution λ_{max} value for **PBB3** was 779 nm, while the thin film absorption maximum was slightly red-shifted at 790 nm with absorption onsets around 850 nm. This represents a significant red shift when compared to **PTB2**,[19] **PTB7**,[17] and **PTBF2**,[24] which showed absorbance maxima between 670 and 683 nm as shown in Table 1. As compared to these other polymers, **PBB3** shows a broader range of absorbance, covering the region from around 500 to 850 nm. Comparatively, **PTB7** showed coverage from 550 to 750 nm; thus, **PBB3** exhibits extended spectral coverage into the near-IR region of almost 100 nm. On the basis of the absorbance onset, **PBB3** showed a narrower optical band gap of 1.44 eV, very close to the ideal value of 1.5 eV.[22] Because our design strategy was to modify the **PTB** series of polymers to reduce the polymer band gap to cover a broader range of the spectrum including absorption in the near-IR range, it would appear based on the optical absorption spectrum that **PBB3** had done exactly that. The solar photon flux reportedly peaks at around 700 nm (1.77 eV);[15] thus, the narrow optical band gap and near-IR coverage of **PBB3** showed promise for OPV applications.

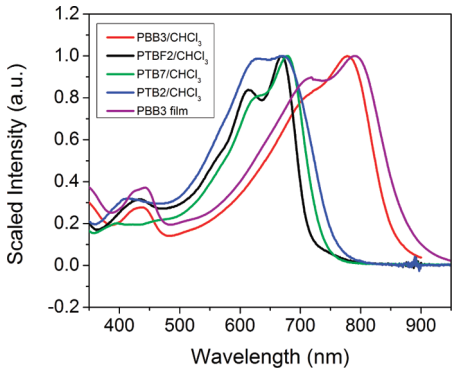

Figure 2. Normalized optical absorption spectra of **PBB3** (chloroform solution, thin film), **PTBF2** (chloroform solution), **PTB7** (chloroform solution), and **PTB2** (chloroform solution).

Table 1. Molecular Weights and Thin-Film Optical Absorption Properties of PBB3 As Compared to PTB2, PTB7, and PTBF2

polymer	M_w (kDa)	PDI	λ_{max}^{film} (nm)	λ_{onset} (nm)	E_g^{opt} (eV)
PTB2[a]	23.2	1.38	683, 630	780	1.59
PTB7[b]	97.5	2.1	671, 628	737	1.68
PTBF2[c]	26.7	2.38	670, 611	709	1.75
PBB3	181.3	1.99	790, 719	863	1.44

[a] Data from ref 19. [b] Data from ref 17. [c] Data from ref 24.

Electrochemical Properties. The electrochemical properties of **PBB3** were investigated using cyclic voltammetry (CV), and the results were compared to those previously reported for **PTB2**, **PTB7**, and **PTBF2**. The positions of the HOMO and LUMO energy levels were calculated as detailed in the Supporting Information from the oxidation and reduction onset potentials of 0.20 and −1.47 eV, respectively. The LUMO energy level for **PBB3** was found to be −3.28 eV, slightly lower than that of **PTB2** (−3.22) as shown in Table 2, and similar to the value of −3.31 eV determined for **PTB7**. The position of the LUMO of the donor material in organic photovoltaic devices is critical because the offset between the LUMO of the donor and the LUMO of the acceptor must be sufficient to drive charge separation. According to Bittner and co-workers,[27] the band offset must be greater than the exciton binding energy; otherwise, the exciton will be the lowest energy excited state and charge separation

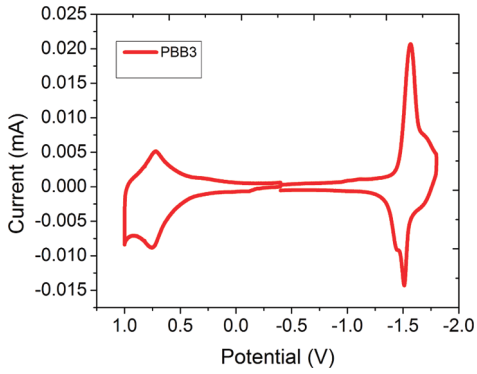

Figure 3. Cyclic voltammogram of **PBB3**.

Table 2. Characteristic Properties of Polymers[a]

polymer	HOMO (eV)	LUMO (eV)	E_g^{elec} (eV)	polymer:PCBM (w/w)	solvent	V_{oc} (V)	J_{sc} (mA/cm^2)	FF (%)	PCE (%)
PTB2:$PC_{61}BM$[b]	−4.94	−3.22	1.72	1:1	DCB	0.58	14.1	62.4	5.1
PTB7:$PC_{71}BM$[c]	−5.15	−3.31	1.84	1:1.5	CB/DIO	0.74	14.5	68.97	7.40
PTBF2:$PC_{71}BM$[b]	−5.41	−3.60	1.81	1:1.5	DCB/DIO	0.68	11.1	42.2	3.20
PBB3:$PC_{61}BM$	−4.95	−3.28	1.67	1:1.5	CB/DIO	0.57	6.51	38.6	1.44
PBB3:$PC_{71}BM$	−4.95	−3.28	1.67	1:1.5	CB/DIO	0.63	6.37	51.0	2.04

[a] HOMO/LUMO energy levels and electrochemical band gap (E_g) for **PBB3** calculated from cyclic voltammogram as shown in Figure 3. CB = chlorobenzene, DCB = 1,2-dichlorobenzene, DIO = 1,8-diiodooctane (3 wt % used). Data shown are best solar cell performance results achieved. [b] Data from ref 24. [c] Data from ref 17.

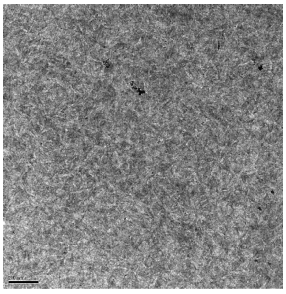

Figure 4. TEM image of **PBB3**:$PC_{61}BM$ 1:1/CB/DIO. Scale bar = 200 nm. CB = chlorobenzene, DIO = 3% 1,8-diiodooctane (v/v).

will not occur at the interface. It is reported that the offset must be at least 0.3 eV[22] to be sufficient to drive charge separation. The LUMO energy level of $PC_{61}BM$ is reported to be −3.70 eV.[20] Our own CV measurements were relatively consistent with this, showing the LUMO levels for $PC_{61}BM$ and $PC_{71}BM$ to be −3.75 and −3.76 eV, respectively. Clearly, the energy offset is sufficient to drive charge separation for all polymers reported herein. The HOMO energy level for **PBB3** (−4.95 eV) was found to be very similar to that of **PTB2** (−4.94 eV), and they also showed nearly identical V_{oc} values as shown in Table 2.

Charge-Carrier Mobility. The charge-carrier mobility of the **PBB3** polymer was measured according to the space charge limited current model (SCLC) as detailed in the Supporting Information. **PBB3** showed a hole mobility of 1.08×10^{-4} $cm^2/(V \cdot s)$ as compared to the values previously reported for **PTB2**, **PTB7**, and **PTBF2** (2.7×10^{-4}, 4.1×10^{-4}, and 1.8×10^{-4}, respectively).

Morphological Properties. The blend film morphology is critical in optimizing exciton diffusion, charge separation, and electron (hole) transfer to cathode (anode). It is reported that the domain size should be on the order of the exciton diffusion length (∼10 nm) due to the limited life of the exciton.[3] Figure 4 shows a TEM image of a **PBB3**/$PC_{61}BM$ blend film prepared using the same conditions as those found to give the best PCE results for **PBB3**. This consisted of a 1:1.5 ratio of polymer:$PC_{61}BM$ spin coated from a 10 mg/mL chlorobenzene solution prepared with 3% (v/v) 1,8-diiodooctane additive. This **PBB3** polymer film possesses both uniform and fine features (approximately 10−20 nm scale), showing nanoscale phase separation as was previously observed for both **PTB2** and **PTB7**. Additionally, the absence of large, spherical domains in the TEM image suggests the formation of a bicontinuous network, which is a morphology conducive to good performance in BHJ devices.

Solar Cell Device Performance. All of the above characteristics indicate that this polymer is very promising for BHJ solar cell applications. The solar cell performance of the **PBB3** polymer was studied in a device with the structure ITO/PEDOT:PSS/polymer:$PC_{71}BM$/Ca/Al. The active layer of polymer was spin-coated from a 10 mg/mL chlorobenzene solution with a small amount of 1,8-diiodooctane additive. The device was prepared from **PBB3** in a weight ratio of 1:1.5 polymer:$PC_{71}BM$. The current density versus voltage ($J-V$) curve was measured under AM 1.5G irradiation at 100 mW/cm^2. The best results are summarized in Table 2. The $J-V$ curve for the best-performing device prepared from **PBB3**:$PC_{71}BM$ is shown in Figure 5. As shown, the highest PCE achieved from **PBB3** was 2.04%, substantially lower than the values achieved

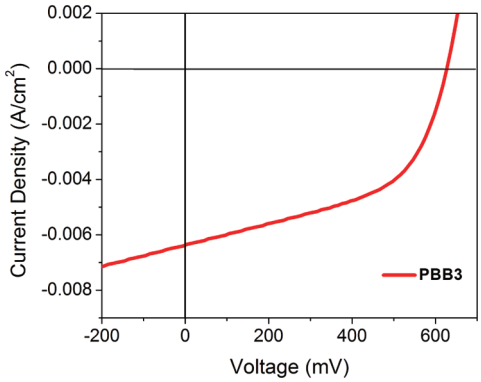

Figure 5. $J-V$ curve obtained from best-performing device based on **PBB3**:$PC_{71}BM$ measured under AM 1.5G at 100 mW/cm^2. Device configuration of ITO/PEDOT/**PBB3**:$PC_{71}BM$(1:1.5)/Ca(20 nm)/Al(80 nm), **PBB3**:$PC_{71}BM$ (1:1.5), active layer spun at 1200 rpm from chlorobenzene (10 mg/mL) with 3% (v/v) 1,8-diiodooctane additive.

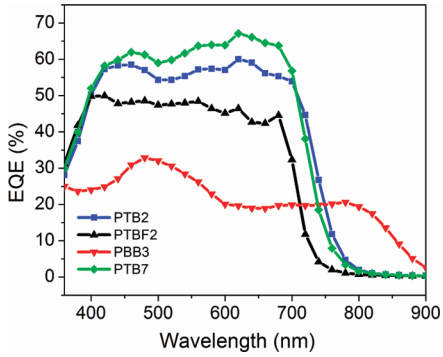

Figure 6. External quantum efficiency data measured for polymer:$PC_{71}BM$ blend films prepared based on optimal solar cell device preparation conditions for each polymer. **PTB2**:$PC_{71}BM$ (1:1), DCB/3% DIO (w/w); **PTB7**:$PC_{71}BM$ (1:1.5), CB/3% DIO (w/w); **PTBF2**:$PC_{71}BM$ (1:1.5), DCB; **PBB3**:$PC_{71}BM$ (1:1.5), CB/3% DIO (w/w). DCB = dichlorobenzene, CB = chlorobenzene, DIO = 1,8-diiodooctane.

from previously reported polymers. As compared to **PTB2**, **PTB7**, and **PTBF2**, the values of FF and J_{sc} for **PBB3** are the most strikingly different.

Given the seemingly optimal conditions observed in the optical absorption spectrum, the comparable values of HOMO and LUMO energy levels determined from cyclic voltammetry, and the morphology shown in the TEM images, it became clear that there must be other factors involved in determining solar cell performance besides those we had already optimized. The most remarkable difference shown is in the J_{sc} where devices based on **PBB3** showed a low value of 6.37 mA cm^{-2}, less than one-half that obtained for **PTB2** and **PTB7** (Table 2). This is most likely the result of its low external quantum efficiency throughout the absorption spectrum as detailed below. Additionally, **PBB3** showed a fill factor of only 51.0% as shown in Table 2.

External Quantum Efficiency. The external quantum efficiency (EQE) for **PTB2**, **PTB7**, **PTBF2**, and **PBB3** was measured, and results are shown in Figure 6. The trend in EQE roughly tracks that observed in overall PCE, in which **PBB3** shows the lowest quantum efficiency and **PTB7** shows the highest. As expected, **PBB3** shows an EQE contribution at wavelengths

Table 3. Calculated Dipole Moments for TT Monomer Components of PTB2, PTB7, PTBF2, and BTT Monomer Component of PBB3[a]

polymer	μ_g (D)	μ_e (D)	μ_{tr} (D)	$\Delta\mu_{ge}$ (D)
PTB2	3.60	6.37	8.50	2.96
PTB7	3.76	7.13	8.23	3.92
PTBF2	3.35	5.45	9.19	2.41
PBB3	0.61	0.82	10.62	0.47
P3HT	0.19	0.43	6.64	0.42

[a] μ_g = ground-state dipole moment, μ_e = excited-state dipole moment, μ_{tr} = transition-state dipole moment, $\Delta\mu_{ge}$ = difference between the ground- and excited-state dipole moments.

between 700 and 800 nm, while the other three polymers do not, which is in keeping with the **PBB3** polymer's red-shifted absorption maximum relative to the other polymers. The device based on **PBB3** shows moderate photoconversion efficiencies (20−30%) throughout the range from 400 to 800 nm. This is substantially lower than the photoconversion efficiencies observed for **PTB7** of more than 60% throughout the 400−700 nm range, and the lowest of the polymer series. The low EQE for **PBB3** throughout the absorption spectrum is consistent with a slow decay in the exciton and fast charge recombination in this system as shown below and explains the low J_{sc} values obtained for the solar cell devices.

Dipole Calculations. The calculated dipole moments for the TT monomer components of **PTB2**, **PTB7**, **PTBF2** and the BTT monomer component of **PBB3** are shown in Table 3, with oscillator strengths and extinction coefficients shown in Table S1 of the Supporting Information. Additionally, the average dipole moments for 1−4 repeat units of the polymer are given in Table S2 of the Supporting Information. Calculations were based on placing the ester groups in two main positions, then averaging the dipole of the two positions with the ester groups oriented 180° relative to one another. To simulate the randomization of the ester positions, the averaged dipole moments for each polymer were determined and used for the analysis of the backbone chain dipole dependence. The dimer of the **PTB7** polymers shows a slightly lower dipole moment because the symmetry of the molecules is slightly increased. The increase of the dipole moment with respect to length is expected for these polymers due to the increase of the polar atoms in the system. The dipole analysis for both the ground and the excited states was determined using the Austin model (AM1) in Hyperchem. For these simulations, the direction of the TT units in the **PBB3** acceptor units was taken from the results in the HNMR spectrum of the monomer, which is shown in the Supporting Information. Both the ground (μ_g = 0.61 D) and the excited state (μ_e = 0.82 D) dipole moments were calculated for **PBB3**. The degree of photoinduced intramolecular charge transfer is related to the difference between the ground- and excited-state dipole moments ($\Delta\mu_{ge}$).[28,29] This number is not to be confused with the transition state dipole (μ_{tr}), which will be discussed further below.

The directionality and amplitude of the local dipole moments of monomer units in **PBB** and nonfluorinated **PTB** are shown in the Supporting Information. The **PBB** monomer shown in Figure S1a of the Supporting Information shows the lowest dipole moment (0.61 D). The direction of the dipole is almost parallel to the direction of the BDT donor unit in the molecule, which indicates that the dipole moment is dominated by this segment of the molecule. The calculated excited-state dipole of the **PBB** monomer is 0.82 D. The directional changes in the dipole moment of the monomers were also analyzed. The dipole moment increased out of the plane of the backbone chain by 0.39 D and decreased in the direction along the backbone chain by 0.21 D. The overall change in the ground- and excited-state dipole $\Delta\mu_{ge}$ was determined by accounting for the changes of the dipole along each coordinate axis:

$$\Delta\mu_{ge} = [(\mu_{gx} - \mu_{ex})^2 + (\mu_{gy} - \mu_{ey})^2 + (\mu_{gz} - \mu_{ez})^2]^{1/2}$$

Using this relationship, $\Delta\mu_{ge}$ is 0.47 D. This change in the dipole moment is very similar to that in **P3HT**, which is also shown in Table 3 for comparison. This suggests that the local donor−acceptor nature of the **PBB** series is reduced due to the trans-conformation of the two TT moieties in the acceptor BTT unit where the electron density pulling directions from the two TT moieties are opposite. In contrast, the nonfluorinated **PTB** monomer analogue (Figure S1a) has the ground- and excited-state dipole moments of 3.6 and 6.37 D, which are significantly larger than that of the **PBB** monomer unit even though they have only one electron-withdrawing TT moiety.

The local dipole of the **PTB** monomer is also oriented more along the TT unit, indicating that the ground-state dipole moment is dominated by the acceptor moiety. The asymmetric single TT unit along with the electron-withdrawing COOMe group draws a more significant amount of electron density into the acceptor moiety. The change in the dipole moment from the ground to the excited state is 3.0 D, which is over 6 times greater as compared to the **PBB** monomer. Furthermore, the greatest change in the dipole moment is directed along the conjugated chain backbone. These calculations indicate the enhanced intramolecular charge transfer properties of the **PTB** series. To further investigate this series, the dipole changes of the **PTB** monomer with varying degrees of fluorination were also calculated. These series are comparable to the aforementioned **PTBF** systems. The largest dipole change is observed in the **PTB7** monomer analogue.

As shown, both **PTBF2** and **PBB3** indicate that the local dipole moment is reduced in one monomer unit of the copolymer as compared to that in **PTB2** and **PTB7**. The reduction effect is most pronounced in **PBB3**, with the dipole moment essentially canceled, while **PTBF2** still maintains a net dipole moment in the TT component. As shown, the least efficient of this series of polymers was **PBB3**, and second least efficient was **PTBF2**. The reduced dipole in the former is due to the cancellation of the electron pulling in the opposite directions by the two TT moieties in a trans-conformation, and the effect in the latter is due to the two fluorine atoms with the electron pulling direction opposite to that of the TT moiety in the monomer. It is possible that the BTT component of the polymer backbone acts as a trapping site, thus preventing full charge separation from occurring. The push−pull concept[14] introduced by Havinga and co-workers has been utilized by many groups across organic photovoltaic research. This consists of pairing a significantly electron-rich "donor" with an electron-deficient "acceptor" comonomer, thus lowering the band gap of the polymer and facilitating intrachain charge transfer.[16,30] Durrant and co-workers[3] reported that the separation of charge occurs through a pathway involving excitation of an electron to an excited state (HOMO−LUMO transition). This is followed by exciton diffusion to the donor/acceptor interface, where a charge

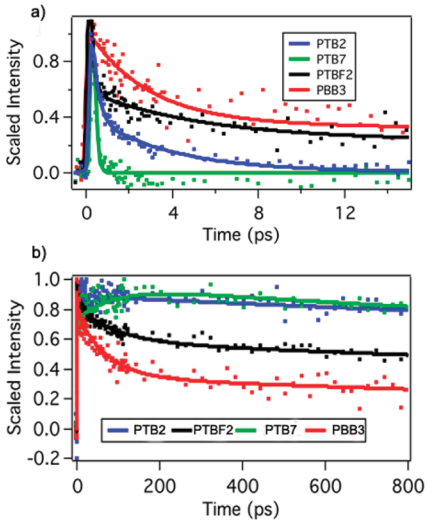

Figure 7. Decay traces for BHJ blended films of **PTB2**, **PTB7**, **PTBF2**, and **PBB3** for (a) the excitonic state and (b) the charge-separated state.

transfer (CT) state formed via charge transfer to an acceptor, wherein the electron and hole, even though primarily existing on different species, are still loosely Coulombically bound. Thus, recombination is still possible. Silva and co-workers[31] found that these so-called charge transfer excitons could act as intrinsic traps for newly photogenerated excitons, and that they showed a long lifetime relative to intrachain excitons. Thus, the Coulombically bound CT excitons limited photocurrent generation in the device. In the **PBB3** polymers, we reasoned that the poor performance may be the result of poor charge separation characteristics, that this may be the result of the minimization of net dipole moment inhibiting charge transfer (facilitating recombination), and that this explains the low J_{sc}, low EQE, and low FF from the device because a similar effect was also observed in **PTBF2**. The **PTBF2** polymer exhibited a minimization of dipole moment in the polymer backbone. It would seem that another factor, the net dipole moment, may be involved in controlling charge transfer in organic photovoltaic polymers. In other words, not only is the interfacial dipole moment in BHJ solar cells critical, but the intrachain dipole moment will also affect charge transfer.

Although the charge transfer characteristics are not optimized in the **PBB** polymer series, the transition dipole moment, and, in turn, the oscillator strength of the transition to the first excited state, is highest. For comparison, the experimental extinction coefficients and oscillator strengths for the polymers are shown in the Supporting Information (Table S1). The oscillator strength is related to the extinction coefficient by the relationship $f \approx 4.31 \times 10^{-9} \int \varepsilon \, d\nu$,[32] where f is the oscillator strength, ε is the extinction coefficient, and ν is the spectral frequency. The experimental results are consistent with the trend of the calculated oscillator strengths for the monomers. The transition dipole is a measure of the overlap between the ground-state and excited-state moments. Therefore, it would follow that the higher changes in dipole moments would lead to a decrease in the overall oscillator strength. Nevertheless, it is interesting to note that even though the light harvesting capability of the **PBB** polymers is very high, the efficiency of the **PBB** OPV devices is still low due to the effects of intramolecular charge transfer within the polymer chains.

Table 4. Thin-Film Electron Transfer Kinetics for PTB2, PTB7, PTBF2, and PBB3[a]

polymer	ex (ps)	ex (%)	CS (ps)	CS (%)
PTB2	<0.12	73	4.9	−11 (rise)
	4.9	27	1500	32
			>3 ns	68
PTB7	<0.12	100	87	−16 (rise)
			>3 ns	100
PTBF2	0.4	81	1.6	17
	19	19	93	23
			>3 ns	60
PBB3	2.8	66	6	15
	190	34	70	51
			>3 ns	34

[a] ex = exciton decay component, CS = charge-separated state.

Transient Absorption Spectroscopy: Effects of the Dipole Moment on the Exicted States. The decay traces for BHJ blended films of **PTB2**, **PTB7**, **PTBF2**, and **PBB3** for (a) the excitonic state and (b) the charge-separated state are shown in Figure 7. The measurement of the decay traces of the excitonic and charge-separated states is detailed in the Supporting Information. The fast decay component of the excitonic state is attributed to the electron transfer from the polymer to the PCBM acceptor molecules. **PTB7** and **PTB2** show the fastest electron transfer rates. The kinetic results are shown in Table 4. The electron transfer kinetics for **PTB7** has one ultrafast decay component with a time constant shorter that the instrument response function of ~120 fs. The excitons in the **PTB2** polymer show ultrafast decay kinetics followed by a 4.9 ps decay. The longer decay component is attributed to the exciton migration to the polymer/PCBM interface. A corresponding 4.9 ps rise time in the charge-separated state was observed, showing the transfer into the charge-separated state. Grazing incidence X-ray experiments have shown enhanced crystallinity in **PTB2** as compared to **PTB7**.[33]

The larger domain size will result in a larger exciton migration component in the **PTB2** polymer. The electron transfer time of the **PTBF2** polymer is 400 fs, which means that the driving force for electron transfer is smaller for this polymer. The **PBB3** molecule shows the slowest electron transfer dynamics in the films. The initial fastest exciton decay component for the **PBB3** polymer is 2.8 ps. A lower driving force for electron transfer could inhibit exciton splitting, which in turn will decrease the population of carriers able to diffuse through the system and to their corresponding electrodes. The **PTBF2** and **PBB3** blended films showed a faster recombination rate of the charge-separated species, further indicating that the electron and holes are more tightly bound in these systems, enhancing the encounters between the two species. Because the initial intramolecular charge separation can be considered a nonadiabatic electron transfer reaction, its rate constant k_{ET} can be described by the Marcus equation for the electron transfer:[3]

$$k_{ET} = \frac{2\pi}{h} H_{DA}{}^2 (4\pi\lambda k_B T)^{-1/2} \exp\left[\frac{-(\Delta G + \lambda)^2}{4\lambda k_B T}\right]$$

where H_{DA} is the electronic coupling matrix between D and A, ΔG is the free energy or the driving force of the reaction, and the total reorganization energy is λ. As an approximation, the driving

force is conventionally determined by the energy difference of the LUMO between the polymers and PCBM, assuming the reorganization energy in films is minimized. However, the energy difference for these two states for the **PBB3**:$PC_{71}BM$ system, which was determined by cyclic voltammetry, was approximately 0.47 eV, which is comparable to or surpasses the exciton binding energy required to overcome the Coulombic potential of the electron and hole pairs. The low optical band gap indicates that the difference of these two energy levels could in fact be smaller. The cyclic voltammetry results reveal similar energetic HOMO and LUMO levels for the **PTB7** and **PBB3** polymers. Therefore, the typical picture of the driving force of these systems breaks down in this comparison. Recently, there has been some controversy regarding the maximized energy levels to promote charge separation. From these results, the following picture emerges: the intramolecular transfer in the polymers will partially separate the charges, which will in turn lower the Coulombic potential between the electron and hole in the system. Therefore, the polymer systems with higher internal dipole moments will need a lower driving force to effectively create charges. The changes in the dipole moment can in effect change the relative interaction region of the electrons and holes in the polymer before injection, meaning that the optimal driving force can vary from polymer to polymer.

The decay of the cationic state is shown in Figure 7. The **PBB3** polymer has the fastest average recombination rate of the charge-separated state. The **PTB2** and **PTB7** polymers do not show an appreciable decay within 1 ns. The **PTB7** shows a rise time that is connected to the charge dissociation in the blended film and will be discussed in future works. A small amount of recombination is observed, but also a long-lived state that cannot be monitored within the time scale of these experiments. On the basis of nanosecond to millisecond TA measurements on conducting polymers, this lifetime is longer by several orders of magnitude than the 3 ns maximum window used in these experiments. The shorter recombination times indicate that the separated charges are not able to effectively overcome the Coulomb interaction between the electron and hole pair. The charge-separated state was also observed in the neat film, but it is not shown here. The kinetics of the charge-separated state in the blended film at early times are comparable to the charge-separated state in the neat film. The electron transfer could be inhibited by low exciton migration rates or rapid transfer to defect states. Larger polymer domain sizes would hinder exciton migration and will be discussed in detail in later works.

From these results, the picture of a dipolar effect emerges. The large local dipole change ($\Delta\mu_{ge}$ (D)) in the single thienothiophene unit in the **PTB** polymers renders the excited state largely polarized. The negative charge will be concentrated on the electron-deficient TT unit. This is a key feature of the donor−acceptor or "push−pull" nature of the polymer.[14] Andersson and co-workers[30] showed that in D−A polymers, the electron resides primarily on the electron-poor component, while the hole resides primarily on the electron-rich component. The concentration of negative charge on the TT unit favors charge transfer to PCBM as evidenced by the fast decay component of the excitonic state shown in Figure 7a, in which **PTB7** and **PTB2** showed the fastest electron transfer rates. After charge separation, the negative charge will be transferred to the PCBM molecule in close contact with the TT unit. The positive charge, however, will be likely to distribute over the electron-rich BDT unit to avoid the dipolar field in the TT unit. This is consistent with the longer lifetime of the cationic species in **PTB7** and **PTB2**, which makes further charge dissociation and transport easier. However, for **PTBF2** polymers, the introduction of two fluorine atoms in the BDT unit makes the BDT unit more electron deficient and less compatible with positive charge. The more positive charge distribution will be forced into the TT units, which will increase the binding energy of the charge transfer complex formed. This leads to enhancement in its recombination decay rate constant, consistent with the faster recombination rate of the charge-separated species in **PTBF2** as shown in Figure 7b. For **PBB3** polymers, a similar reason exists except that the BTT unit has an almost canceled dipole moment, and thus the electron density in the BTT conjugated system remains very high (the BTT moiety contains 20 π-electrons over 16 atoms). Thus, it will be more accommodative to positive charge, resulting in a strong binding force with negative charge in the neighboring PCBM molecule. Consistent with this, the charge recombination rate is the highest among all of the polymers discussed. Thus, the solar cells from this polymer have the smallest J_{sc}, lowest EQE, and lowest PCE, although all of the materials characteristics are seemingly optimal. Notably, our modeling studies of the dipole moment of monomer units as shown in Table 3 indicate that **PBB3** shows a dipole moment very similar to that of **P3HT**. Significantly, while PCE's of close to 5% have been achieved from **P3HT**,[34] the efficiencies of optimally processed **P3HT** are still much lower than those of the **PTB** series, as well as several recent examples from the literature, the high efficiencies (∼7%) of which seem to support the incorporation of comonomers bearing a substantial net dipole moment in the polymer backbone.[35−38] A possible explanation for this is that **P3HT** displays a much greater degree of crystallinity,[5] improving its efficiency due to increased exciton diffusion length. Our recent work showed that the crystallinity of **PTB7** is only about 18%, much smaller than **P3HT**, yet its solar cell efficiency is much higher.[39] Of course, it is important to emphasize that while a dipolar effect seems to be consistent with the evidence presented herein, it is not the only effect present in OPV polymers, and a number of parameters must be synergistically optimized to achieve high PCE.

■ CONCLUSIONS

The synthesis and characterization of the **PBB3** polymer revealed the importance of the presence of a local dipole moment in repeating units of low band gap polymers. While the features such as HOMO and LUMO energy level matching with PCBM acceptors, thin film morphology, and band gap were seemingly optimal, the performance of solar cell devices based on this polymer was significantly lower than expected. We rationalized this effect based on the minimized dipole moment in the polymer backbone of the **PBB3** polymer when compared to the high-efficiency **PTB7** polymer. The large, localized change in the dipole moment in the single TT unit in polymers such as **PTB7** renders the excited state highly polarized when compared to that of **PBB3**; thus, negative charge tends to be concentrated in this unit while the positive charge tends to be concentrated in the electron-rich BDT unit. This facilitates electron transfer to the PCBM acceptor. Conversely, in the **PBB3** polymers, the minimized dipole moment favors trapping of positive charge in the BTT dimer, thus leading more readily to recombination. The faster recombination rate of the charge-separated species indicates a greater binding energy in these species; thus, charge separation is more difficult. The success of a number of polymer

systems reported in the recent literature underscores the importance of incorporating a net dipole moment into the backbone of new polymers in the rational design of new systems for organic solar cells.

■ ASSOCIATED CONTENT

Supporting Information. Experimental details for the syntheses of new compounds, characterization data for all new compounds, complete dipole calculations, oscillator strengths and extinction coefficients, instruments, measurements, fabrication of solar cell devices, as well as relevant transient absorption spectral data. This material is available free of charge via the Internet at http://pubs.acs.org.

■ AUTHOR INFORMATION

Corresponding Author
lchen@anl.gov; lupingyu@uchicago.edu

■ ACKNOWLEDGMENT

We gratefully acknowledge support of this work by the NSF (NSF DMR-1004195), AFOSR and NSF MRSEC program at the University of Chicago, and DOE via the ANSER Center, an Energy Frontier Research Center funded by the U.S. Department of Energy, Office of Science, Office of Basic Energy Sciences, under award number DE-SC0001059.

■ REFERENCES

(1) Brabec, C. J.; Sariciftci, N. S.; Hummelen, J. C. *Adv. Funct. Mater.* **2001**, *11*, 15.
(2) Cheng, Y.; Yang, S.; Hsu, C. *Chem. Rev.* **2009**, *109*, 5868.
(3) Clarke, T. M.; Durrant, J. R. *Chem. Rev.* **2010**, *110*, 6736.
(4) Sariciftci, N. S.; Smilowitz, L.; Heeger, A. J.; Wudl, F. *Science* **1992**, *258*, 1474.
(5) Ohkita, H.; Cook, S.; Astuti, Y.; Duffy, W.; Tierney, S.; Zhang, W.; Heeney, M.; McCulloch, I.; Nelson, J.; Bradley, D. D. C.; Durrant, J. R. *J. Am. Chem. Soc.* **2008**, *130*, 3030.
(6) Yu, G.; Gao, J.; Hummelen, J. C.; Wudl, F.; Heeger, A. J. *Science* **1995**, *270*, 1789.
(7) Li, G.; Shrotriya, V.; Huang, J.; Yao, Y.; Moriarty, T.; Emery, K.; Yang, Y. *Nat. Mater.* **2005**, *4*, 864.
(8) Li, G.; Chu, C.; Shrotriya, V.; Huang, J.; Yang, Y. *Appl. Phys. Lett.* **2006**, *88*, 253503.
(9) Li, G.; Yao, Y.; Yang, H.; Shrotriya, V.; Yang, G.; Yang, Y. *Adv. Funct. Mater.* **2007**, *17*, 1636.
(10) Roncali, J. *Chem. Rev.* **1997**, *97*, 173.
(11) Winder, C.; Sariciftci, N. S. *J. Mater. Chem.* **2004**, *14*, 1077.
(12) Bundgaard, E.; Krebs, F. C. *Sol. Energy Mater. Sol. Cells* **2007**, *91*, 954.
(13) Thompson, B. C.; Fréchet, J. M. J. *Angew. Chem., Int. Ed.* **2008**, *47*, 58.
(14) Havinga, E. E.; Ten, H. W.; Wynberg, H. *Polym. Bull.* **1992**, *29*, 119.
(15) Dhanabalan, A.; Van, D.; Jeroen, K. J.; Van, H.; Paul, A.; Van, D.; Joost, L. J.; Janssen, R. A. J. *Adv. Funct. Mater.* **2001**, *11*, 255.
(16) Jespersen, K. G.; Beenken, W. J. D.; Zaushitsyn, Y.; Yartsev, A.; Andersson, M.; Pullerits, T.; Sundstrom, V. *J. Chem. Phys.* **2004**, *121*, 12613.
(17) Liang, Y. Y.; Xu, Z.; Xia, J.; Tsai, S.; Wu, Y.; Li, G.; Ray, C.; Yu, L. P. *Adv. Mater.* **2010**, *22*, E135.
(18) Liang, Y. Y.; Yu, L. P. *Acc. Chem. Res.* **2010**, *43*, 1227.
(19) Liang, Y. Y.; Feng, D.; Wu, Y.; Tsai, S.; Li, G.; Ray, C.; Yu, L. P. *J. Am. Chem. Soc.* **2009**, *131*, 7792.
(20) Liang, Y. Y.; Wu, Y.; Feng, D.; Tsai, S.; Son, H.; Li, G.; Yu, L. P. *J. Am. Chem. Soc.* **2009**, *131*, 56.
(21) Liang, Y. Y.; Xiao, S.; Feng, D.; Yu, L. P. *J. Phys. Chem. C* **2008**, *112*, 7866.
(22) Scharber, M. C.; Muehlbacher, D.; Koppe, M.; Denk, P.; Waldauf, C.; Heeger, A. J.; Brabec, C. J. *Adv. Mater.* **2006**, *18*, 789.
(23) Kooistra, F. B.; Knol, J.; Kastenberg, F.; Popescu, L. M.; Verhees, W. J. H.; Kroon, J. M.; Hummelen, J. C. *Org. Lett.* **2007**, *9*, 551.
(24) Son, H. J.; Wang, W.; Xu, T.; Liang, Y. Y.; Wu, Y.; Li, G.; Yu, L. P. *J. Am. Chem. Soc.* **2011**, *133*, 1885.
(25) Carsten, B.; He, F.; Son, H. J.; Xu, T.; Yu, L. P. *Chem. Rev.* **2011**, *111*, 1493.
(26) He, F.; Wang, W.; Chen, W.; Xu, T.; Darling, S. B.; Strzalka, J.; Liu, Y.; Yu, L. P. *J. Am. Chem. Soc.* **2011**, *133*, 3284.
(27) Bittner, E. R.; Ramon, J. G. S.; Karabunarliev, S. *J. Chem. Phys.* **2005**, *122*, 214719.
(28) Dehu, C.; Meyers, F.; Bredas, J. L. *J. Am. Chem. Soc.* **1993**, *115*, 6198.
(29) De, H.; Matthijs, P.; Warman, J. M. *Chem. Phys.* **1982**, *73*, 35.
(30) Svensson, M.; Zhang, F.; Veenstra, S. C.; Verhees, W. J. H.; Hummelen, J. C.; Kroon, J. M.; Inganaes, O.; Andersson, M. R. *Adv. Mater.* **2003**, *15*, 988.
(31) Gelinas, S.; Pare-Labrosse, O.; Brosseau, C.; Albert-Seifried, S.; McNeill, C. R.; Kirov, K. R.; Howard, I. A.; Leonelli, R.; Friend, R. H.; Silva, C. *J. Phys. Chem. C* **2011**, *115*, 7114.
(32) Hammond, V. J.; Price, W. C. *Trans. Faraday Soc.* **1955**, *51*, 605.
(33) Szarko, J. M.; Guo, J.; Liang, Y. Y.; Lee, B.; Rolczynski, B. S.; Strzalka, J.; Xu, T.; Loser, S.; Marks, T. J.; Yu, L. P.; Chen, L. *Adv. Mater.* **2010**, *22*, 5468.
(34) Reyes-Reyes, M.; Kim, K.; Carroll, D. L. *Appl. Phys. Lett.* **2005**, *87*, 083506.
(35) Chu, T.; Lu, J.; Beaupre, S.; Zhang, Y.; Pouliot, J.; Wakim, S.; Zhou, J.; Leclerc, M.; Li, Z.; Ding, J.; Tao, Y. *J. Am. Chem. Soc.* **2011**, *133*, 4250.
(36) Zhang, Y.; Zou, J.; Yip, H.; Chen, K.; Zeigler, D. F.; Sun, Y.; Jen, A. K. *Chem. Mater.* **2011**, *23*, 2289.
(37) Piliego, C.; Holcombe, T. W.; Douglas, J. D.; Woo, C. H.; Beaujuge, P. M.; Fréchet, J. M. J. *J. Am. Chem. Soc.* **2010**, *132*, 7595.
(38) Amb, C. M.; Chen, S.; Graham, K. R.; Subbiah, J.; Small, C. E.; So, F.; Reynolds, J. R. *J. Am. Chem. Soc.* **2011**, *133*, 10062.
(39) Hammond, M. R.; Kline, R. J.; Herzing, A. A.; Richter, L. J.; Germack, D. S.; Ro, H.; Soles, C. L.; Fischer, D. A.; Xu, T.; Yu, L. P.; Toney, M. F.; DeLongchamp, D. M. *ACS Nano* **2011**, *5*, 8248.